24 July 2002

Chemical Physics Letters 361 (2002) 169–174

CHEMICAL PHYSICS LETTERS

www.elsevier.com/locate/cplett

Radial breathing modes of multiwalled carbon nanotubes

Xinluo Zhao [a], Yoshinori Ando [a,*], Lu-Chang Qin [b], Hiromichi Kataura [c], Yutaka Maniwa [c], Riichiro Saito [d]

[a] *Department of Materials Science and Engineering, Meijo University, Shiogamaguchi, 1-501, Tempaku-ku, Nagoya 468-8502, Japan*
[b] *JST-ICORP Nanotubulite Project, NEC Corporation, Tsukuba 305-8501, Japan*
[c] *Department of Physics, Tokyo Metropolitan University, Tokyo 192-0397, Japan*
[d] *Department of Electronic Engineering, University of Electro-Communications, Tokyo 182-8585, Japan*

Received 2 May 2002; in final form 3 June 2002

Abstract

A number of Raman-active peaks in the low-frequency region (100–600 cm^{-1}) were observed for multiwalled carbon nanotubes (MWNTs). They were confirmed to be the radial breathing modes (RBMs) by using polarized Raman scattering. These RBMs originate from very thin innermost tubes (diameter, $d = \sim 1$ nm) included in MWNTs, and the RBM peak of the smallest carbon nanotubes ($d = 0.4$ nm) appears at 570 cm^{-1}. It has also been found that the innermost-diameter distribution calculated from the RBM frequencies agrees well with the observations of high-resolution transmission electron microscopy. This provides a new Raman-spectroscopy-based method for the determination of the innermost diameter of MWNTs.

1. Introduction

Multiwalled carbon nanotubes (MWNTs) have unique nanostructure with remarkable properties, and can be used as nanoprobes in a scanning probe microscope (SPM), field electron emitter in super-high luminance light-source. In view of both future technological applications and scientific studies, it is of primary interest to make a precise characterization of the MWNT samples. High-resolution transmission electron microscopy (HRTEM) is so far the only tool for measuring the innermost diameter of MWNTs, although this kind of direct investigation is a rather time-consuming and expensive procedure.

Radial breathing mode (RBM) in Raman spectra is unique to cylindrical symmetry, and has been widely used to determine the diameter of single-walled carbon nanotube (SWNT) [1–3]. Since an ideal MWNT can be considered as consisting of multiple coaxial SWNTs of ever-increasing diameter about a common axis, it can be expected to observe the RBMs from MWNTs. In the past decade, extensive Raman experiments have been performed on the MWNTs, which were synthesized by arc discharge evaporation in helium gas and by chemical vapor deposition (CVD). However, the reported Raman spectra closely resemble that of graphite, and no RBMs have yet been found [4–6] except by Jantoljak et al. [7].

* Corresponding author. Fax: +81-52-832-1170.
E-mail address: yando@ccmfs.meijo-u.ac.jp (Y. Ando).

0009-2614/02/$ - see front matter
PII: S0009-2614(02)00955-7

On the other hand, we observed many Raman-active modes [8] in the low-frequency region (100–600 cm^{-1}) on the MWNTs samples prepared by hydrogen arc discharge [9] and found that the resonance effect of each mode [10] was similar to that of RBM in SWNT. In the present study, we have confirmed that the observed Raman-active modes are the RBMs of MWNTs originating from the very thin innermost tubes included in MWNTs. We have also found that the distribution of innermost diameters calculated from the RBM frequencies is consistent with the observations of HRTEM. This provides a new method for determining the innermost diameter of MWNTs.

2. Experimental

Pristine MWNTs with only a few carbon nanoparticles were prepared by DC arc discharge evaporation (arc current 50 A) of graphite rods in pure hydrogen gas (8.0×10^3 Pa) [9]. Then, we removed the coexisting carbon nanoparticles and purified the pristine MWNTs by infrared irradiation in air at 500 °C for 30 min [11]. The purified material contains more than 95% MWNTs and appears as a sponge with a surface area of the order of 10 mm^2 and a thickness of 0.1 mm in scanning electron microscopy (SEM) images. The X-ray diffraction measurements reveal that the thin MWNTs with the outermost diameter less than 10 nm have a Russian doll structure [12].

Both the outermost and innermost diameters of MWNTs have been investigated by HRTEM. It has been found that the histogram of outermost-diameter distribution of MWNTs has a maximum at 10 nm as shown in Fig. 1, and most of the MWNTs possess very thin innermost diameters of ~1 nm [9]. Raman spectra were obtained using a Raman spectrometer at 514.5 nm (Ar^+ laser: 2.41 eV) with a typical resolution of ~2 cm^{-1} and collected in backscattering geometry at room temperature. The use of 100× microscope objective lens and a TV monitor made it possible to observe the MWNT bundles (length greater than 5 μm). The laser spot had a diameter of ~1 μm at the sample with a power density of ~10^6 W/cm^2.

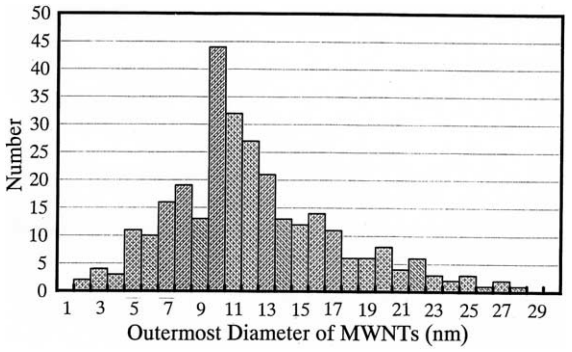

Fig. 1. Histogram of the outermost-diameter distribution of H_2-arc MWNTs obtained from HRTEM.

3. Results and discussion

Fig. 2 shows the micro-Raman spectra in the low-frequency region (100–600 cm^{-1}) for three specimens of MWNT mats, (A)–(C). These MWNT mats were prepared by pressing the sponge of purified MWNTs with a spatula. For comparison, Raman spectra of SWNTs produced

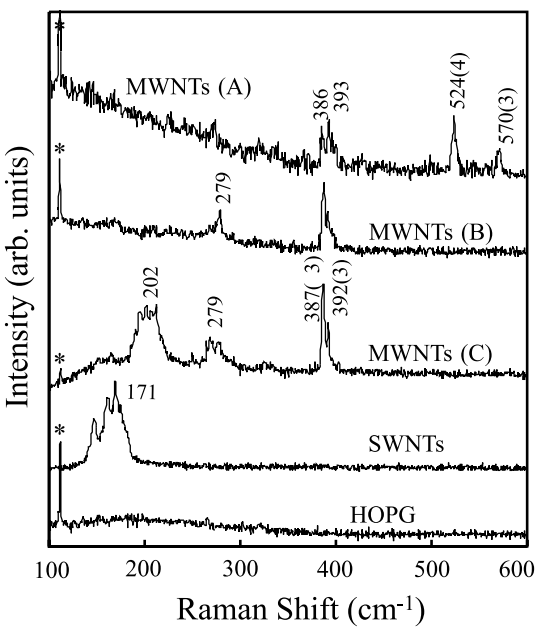

Fig. 2. Micro-Raman spectra in low-frequency region (100–600 cm^{-1}) for three specimens of MWNT mats, (A)–(C). For comparison, Raman spectra of SWNTs and HOPG are also displayed.

by the arc plasma jet method [13] and highly oriented pyrolytic graphite (HOPG) are also displayed in Fig. 2. In contrast to HOPG, which has no peaks in this region except for the sharp peaks labeled "*" attributed to instrumental artifacts, many Raman-active peaks are observed in the Raman spectra of the MWNT mats. There are two peaks having frequencies higher than 500 cm^{-1}. One is the highest frequency peak at 570(3) cm^{-1} in MWNTs (A), where the full-width at half maximum (FWHM) is given in parentheses, and the other is at 524(4) cm^{-1} in the same spectrum. The peaks at about 392(3), 387(3), and 279 cm^{-1} can be observed in all of the Raman spectra for the three MWNT mats. Comparison of the peaks at about 202 cm^{-1} in MWNTs (C) with the peaks at 171 cm^{-1} in SWNTs, which are known to be the RBMs of SWNTs [13,14], shows that their spectral shapes are similar to each other.

Since the low-frequency region in the Raman spectra is a silent region for graphite and other carbon materials, as seen in the HOPG spectrum of Fig. 2, the observed Raman-active peaks should originate from MWNTs. As mentioned above, the He-arc MWNTs [4,7] with the innermost diameter larger than 2 nm have no regular Raman-active peaks in the same region. Therefore, the peaks should be attributed to the thin tubes with diameters less than 2 nm in H_2-arc MWNTs. According to the theory on SWNTs, three Raman-active modes exist in the low-frequency region (100–600 cm^{-1}): E_{1g}, E_{2g} and A_{1g} (armchair and zigzag) [or E_1, E_2 and A_1 (chiral)] [2,15]. The RBM, in which all carbon atoms undergo equal radial displacement, belongs to the A_{1g} (A_1) mode and has a much higher intensity than the other modes. The different polarization selection rule [2] of these three Raman-active modes enables us to assign the observed Raman-active peaks using the polarized Raman scattering technique.

Fig. 3 shows the typical polarized Raman spectra of MWNTs. These spectra were obtained from straight bundles of purified MWNTs sprayed on a silver surface to give surface-enhanced Raman spectra (SERS). The inset in Fig. 3 is a SEM micrograph of a purified MWNT bundle on a SERS substrate, representing a MWNT bundle oriented along the *Z*-direction and the light propagated along the *Y*-direction. We collected the polarized Raman spectra of four configurations, (*ZZ*), (*ZX*), (*XX*) and (*XZ*) polarization geometry, where the letters indicate the polarization directions of the (incident, scattered) light. However, no signals were detected in (*XX*) and (*XZ*) polarization geometry. We display the Raman spectra of (*ZZ*) and (*ZX*) polarization geometry in Fig. 3. As seen in this figure, six peaks, 163, 171, 197, 209, 267 and 387 cm^{-1}, can be observed in the (*ZZ*) polarization geometry, but they disappear in the (*ZX*) polarization geometry. According to the polarization selection rule of the Raman-active modes in the low-frequency region, the RBM is allowed in the (*ZZ*) configuration, but it is forbidden in the (*ZX*) configuration; the E_1 (E_{1g}) mode is allowed in the (*ZX*) configuration while the E_2 (E_{2g}) mode is allowed only in the (*XX*) configuration [2]. Therefore, each Raman-active peak appearing in Fig. 3 can be assigned to RBM. We performed the same polarized Raman experiments on different straight bundles of purified MWNTs and found that all the observed Raman-active peaks correspond to RBMs, not E symmetries.

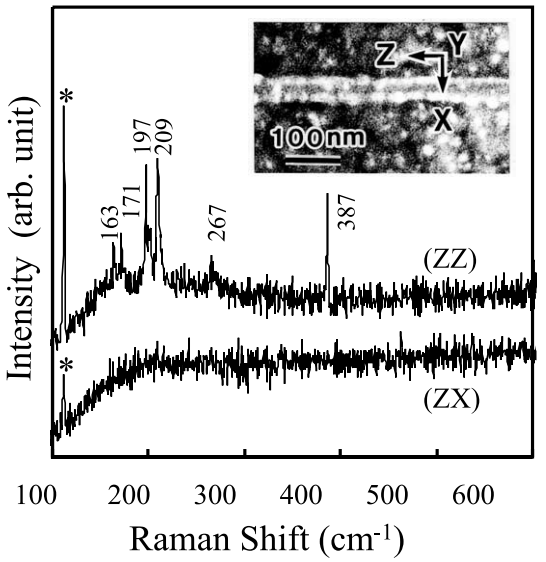

Fig. 3. Polarized Raman spectra of oriented MWNTs. The inset is a SEM micrograph of a purified MWNT bundle on SERS substrate, representing a MWNT bundle oriented along the *Z*-direction and light propagated along the *Y*-direction.

The isolated SWNT diameter is inversely proportional to the RBM frequency [3], $d = 223.75/\omega$, where d is the isolated SWNT diameter in nanometers and ω the RBM frequency in wavenumbers. When SWNTs are arranged on a triangular lattice to form a rope, their RBM frequencies increase 5–10% compared to the isolated one because of van der Waals interaction between SWNTs in the rope [15–17]. In the case of MWNTs, with the help of resonance Raman scattering (RRS) technique, we found by comparing the RBMs of MWNTs with those of SWNTs that the RBM frequencies of MWNTs were up-shifted ~5% due to the interlayer interaction [10].

In regard to the highest frequency of RBM at 570(3) cm^{-1} in MWNTs (A) of Fig. 2, the Lorentzian line shape and the very narrow FWHM of 3 cm^{-1} indicate that the Raman scattering originates from a single tube. Using the relationship between the isolated SWNT diameter and the RBM frequency and taking into account the 5% up-shift, we can determine the diameter of this tube to be $d = 0.41$ nm. This is the smallest carbon nanotube according to the theoretical calculation [18]; it has been observed as the innermost tube inside MWNTs [19]. Because of the interlayer distance of 0.34 nm in MWNTs, when a MWNT contains the smallest carbon nanotube, the MWNT should possess three tubes whose diameters are less than 2 nm: the innermost tube with $d = 0.41$ nm (RBM, 570 cm^{-1}), second cylinder with $d = 1.09$ nm (RBM, 216 cm^{-1}) and third cylinder $d = 1.77$ nm (RBM, 133 cm^{-1}). However, except for 570 cm^{-1} as mentioned above, no RBMs are found at about 216 and 133 cm^{-1} in MWNTs (A) of Fig. 2. This means that we observed the RBM of the innermost tube only. In fact, our RRS study of MWNTs using several laser lines between 1.62 and 2.73 eV showed that in the case of MWNTs only the RBMs of the innermost tubes had a considerable Raman intensity [10]. Furthermore, our SERS study also provides strong support to the above conclusion because we have measured a single RBM for each individual MWNT [20].

In the case of MWNTs, only the innermost tube is in a similar situation to the SWNT rope. The existence of interlayer tubes does not change its cylindrical symmetry, and only provide a long-range van der Waals-type interlayer interaction. Therefore, if the innermost tube diameter is less than 2 nm, its RBM will be observed by using an appropriate laser source, but with an up-shifted frequency due to the interlayer interaction. Because the highly defective CVD MWNTs have an innermost diameter larger than 3 nm, no RBMs have ever been observed. On the other hand, the main difference between He-arc MWNTs and H_2-arc MWNTs is that most of H_2-arc MWNTs possesses very thin innermost diameter of ~1 nm [9], and the sample of He-arc MWNTs have few MWNTs with an innermost diameter less than 2 nm [21]. That is the reason why Jantoljak et al. [7] can observe only a few peaks at special positions on the He-arc MWNT sample. In the case of H_2-arc MWNTs, this provides a new practical method for measuring the innermost diameters of MWNTs. In Fig. 2, the RBMs at 524(4) cm^{-1} in MWNTs (A), 392(3) and 387(3) cm^{-1} in (C), and 279 cm^{-1} in (B) originate from the H_2-arc MWNTs with the innermost diameters of 0.45, 0.60, 0.61 and 0.84 nm, respectively.

More than 40 micro-Raman spectra for H_2-arc MWNTs were detected and a large number of RBMs were recorded. Fig. 4a shows a histogram of the innermost-diameter distribution of H_2-arc MWNTs calculated from the frequencies of RBMs, which we have measured using micro-Raman, RRS and SERS. The discrete peaks can be observed at 4.0, 4.4, 4.8, 5.4, 6.0 and 7.2 Å, and the highest peak appears at 6.0 Å. The reason why the highest peak appears at 6.0 Å can be explained by the resonant Raman effects of RBMs originating from the innermost tubes [10]. The resonance occurs with optical transitions between van Hove singularities in the 1D electronic density of states of the innermost tubes in H_2-arc MWNTs. When an Ar^+ laser (2.41 eV) was used as a light source, the RBMs at about 387 cm^{-1} always showed maximum intensity.

Fig. 4b shows a histogram of the innermost diameters measured from many HRTEM micrographs of H_2-arc MWNTs, where the inset is that of the innermost-diameter range of less than 8 Å. A comparison of the inset in Fig. 4b with Fig. 4a shows that the histograms of the innermost-diameter distributions of H_2-arc MWNTs obtained

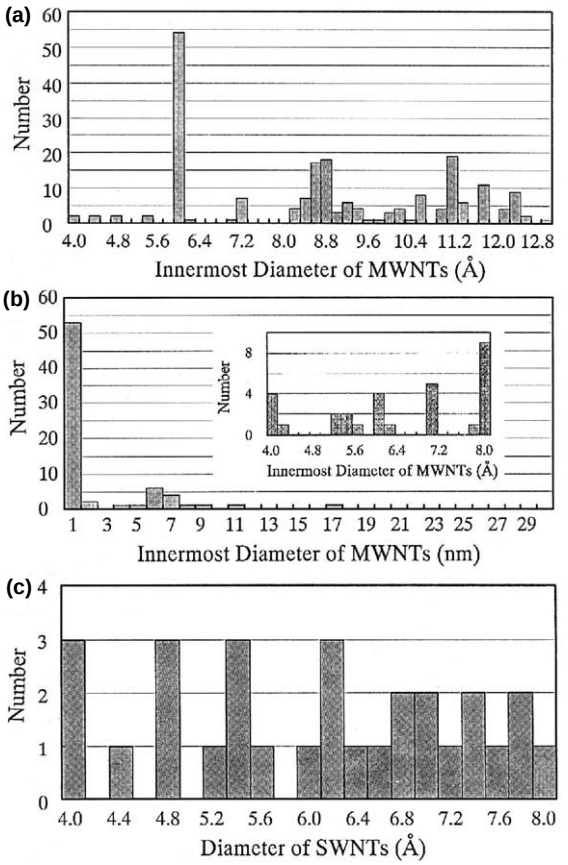

Fig. 4. (a) Histogram of the innermost-diameter distribution of H_2-arc MWNTs calculated from RBM frequencies. (b) Histogram of the innermost-diameter distribution of H_2-arc MWNTs obtained from HRTEM. The inset shows the range less than 8 Å. (c) Histogram of diameter distribution of SWNTs calculated from the chiral vector map for SWNTs.

from both Raman spectroscopy and HRTEM clearly agree with each other in the innermost-diameter range less than 8 Å. Furthermore, we also find that our experimental results from Raman spectroscopy and HRTEM are both consistent with the histogram (see Fig. 4c) calculated from the chiral vector map. Therefore, it is convincible that the RBM frequencies of MWNTs are upshifted ~5% by the interlayer interaction.

4. Conclusions

Using polarized Raman scattering studies performed on a single straight bundle of H_2-arc MWNTs, we have confirmed that the Raman-active modes observed in the low-frequency region (100–600 cm^{-1}) are all the RBMs of MWNTs. We draw the conclusion that they originate from the very thin innermost tubes included in H_2-arc MWNTs, and that we have observed the RBM peak of the smallest carbon nanotubes at 570 cm^{-1}. By a comparison of the innermost-diameter distribution calculated from RBM frequencies with the observation results of HRTEM, we have further set forth a new method of Raman-spectroscopy-based measurement for determining the innermost diameter of MWNTs. This enables characterization of MWNTs incorporated in a nanoscale device by using instrument for surface analysis such as a Raman spectrometer and SPM.

Acknowledgements

We thank Mr. M. Takizawa, Dr. S. Bandow and Dr. M. Hiramatsu for their help and discussions concerning Raman experiments. This work was partially supported by the Grant-in-Aid (No. 11165240) for Scientific Research on the Priority Area 'Fullerenes and Nanotubes' by the Ministry of Education, Culture, Sports, Science and Technology, Japan. X.Z. is grateful for the JSPS Postdoctoral Fellowship, and R.S. acknowledges a Grant-in-Aid (No. 13440091) from the Ministry of Education, Culture, Sports, Science and Technology, Japan.

References

[1] R.A. Jishi, L. Venkataraman, M.S. Dresselhaus, G. Dresselhaus, Chem. Phys. Lett. 209 (1993) 77.
[2] R. Saito, T. Takeya, T. Kimura, M.S. Dresselhaus, G. Dresselhaus, Phys. Rev. B 57 (1998) 4145.
[3] S. Bandow, S. Asaka, Y. Saito, A.M. Rao, L. Grigorian, E. Richter, P.C. Eklund, Phys. Rev. Lett. 80 (1998) 3779.
[4] P.C. Eklund, J.M. Holden, R.A. Jishi, Carbon 33 (1995) 959.
[5] W. Li, H. Zhang, C. Wang, Y. Zhang, L. Xu, K. Zhu, S. Xie, Appl. Phys. Lett. 70 (1997) 2684.
[6] A.M. Rao, A. Jorio, M.A. Pimenta, M.S.S. Dantas, R. Saito, G. Dresselhaus, M.S. Dresselhaus, Phys. Rev. Lett. 84 (2000) 1820.

[7] H. Jantoljak, J.-P. Salvetat, L. Forró, C. Thomsen, Appl. Phys. A 67 (1998) 113.
[8] X. Zhao, Y. Ando, Jpn. J. Appl. Phys. 37 (1998) 4846.
[9] X. Zhao, M. Ohkohchi, M. Wang, S. Iijima, T. Ichihashi, Y. Ando, Carbon 35 (1997) 775.
[10] H. Kataura, Y. Achiba, X. Zhao, Y. Ando, Mat. Res. Soc. Symp. Proc. 593 (2000) 113.
[11] Y. Ando, X. Zhao, Jpn. J. Appl. Phys. 37 (1998) L61.
[12] Y. Maniwa, R. Fujiwara, H. Kira, H. Tou, E. Nishibori, M. Takata, M. Sakata, A. Fujiwara, X. Zhao, S. Iijima, Y. Ando, Phys. Rev. B 64 (2001) 073105.
[13] Y. Ando, X. Zhao, K. Hirahara, K. Suenaga, S. Bandow, S. Iijima, Chem. Phys. Lett. 323 (2000) 580.
[14] A.M. Rao, E. Richter, S. Bandow, B. Chase, P.C. Eklund, K.A. Williams, S. Fang, K.R. Subbaswamy, M. Menon, A. Thess, R.E. Smalley, G. Dresselhaus, M.S. Dresselhaus, Science 275 (1997) 187.
[15] D. Kahn, J.P. Lu, Phys. Rev. B 60 (1999) 6535.
[16] U.D. Venkateswaran, A.M. Rao, E. Richter, M. Menon, A. Rinlzer, R.E. Smalley, P.C. Eklund, Phys. Rev. B 59 (1999) 10928.
[17] L. Henrard, E. Hernández, P. Bernier, A. Rubio, Phys. Rev. B 60 (1999) R8521.
[18] S. Sawada, N. Hamada, Solid State Commun. 83 (1992) 917.
[19] L.-C. Qin, X. Zhao, K. Hirahara, Y. Miyamoto, Y. Ando, S. Iijima, Nature 408 (2000) 50.
[20] X. Zhao, Y. Ando, L.-C. Qin, H. Katauara, Y. Maniwa, R. Saito, Appl. Phys. Lett., in press.
[21] H. Hiura, Mol. Cryst. Liq. Cryst. 267 (1995) 267.